

# In Situ Homeotropic Alignment of Nematic Liquid Crystals Based on Photoisomerization of Azo-Dye, Physical Adsorption of Aggregates, and Consequent Topographical Modification

Sudarshan Kundu, Myong-Hoon Lee, Seung Hee Lee,\* and Shin-Woong Kang\*

The control of the alignment of liquid crystal (LC) is a classic but essential issue in the field of LC research. The fundamental mechanism behind LC alignment has been a controversial argument for a long period of time since early twentieth century. New techniques have been developed for various applications of liquid crystals.<sup>[1]</sup> Both the physical interactions between an elastic LC medium and a solid surface, and the chemical interactions attributed to the epitaxial growth of LC order from the chemically anisotropic surface are generally accepted for the origin of LC alignment.<sup>[1,2]</sup> Either planar or homeotropic alignment, where the easy axis of a nematic director aligned in the plane of a surface or normal to a surface, respectively, is an essential requirement for various device applications. Especially, the techniques for a homeotropic alignment attract a great attention because not only for scientific reason but also for high end television applications of liquid crystal display (LCD).<sup>[1,3]</sup> Although various methods such as a physical adsorption of ionic surfactants, self-assembled monolayer, evaporation deposition of SiO<sub>x</sub>, 2D-topographic patterns have been reported, the polyimide coating with a long hydrocarbon side chain is known as the most reliable and cost-effective process.<sup>[1,3-6]</sup> Covalently attached photochromic azo-benzene moiety on the side chain polymers or glass surfaces can induce a homeotropic alignment and facilitate anchoring transition from the initial homeotropic to the planar state upon irradiation of UV-light due to the *trans*- to *cis*- isomerization of the azo-chromophore (so called, command surface).<sup>[7]</sup> Photochromic azo-benzene derivatives have also been used for a control of homogeneous planar and homeotropic alignment.<sup>[8]</sup> W. M. Gibbons et al. have reported the photoalignment of nematic LCs based on the photochromic behavior of azo-compound. The molecular reorientation of elongated dye molecules caused by intensive polarized light induces an orientational anisotropy of dye molecules and is responsible for homogeneous planar anchoring of LC molecules at the

surface. In this case, molecular reorientation of the azo-dye is a primary factor rather than a *trans*-to-*cis* isomerization.<sup>[8]</sup> Ruslim and Komitov reported a photoinduced homeotropic alignment by using high content liquid crystalline azo-dye.<sup>[8]</sup> In this report, a molecular adsorption of the dye due to a strong dipole-dipole interaction and hydrogen bonding between dye-molecule and polar solid surface were proposed. Subsequent steric interaction between vertically aligned alkyl chain of the *cis*-form dye and LC-molecule is a primary factor for LC alignment.<sup>[8]</sup>

The common feature of all these methods is a pretreatment of substrates for LC alignment and subsequent LC loading. It requires separate processes for alignment and injection of LCs. It is very recent report that nano-particle doped LCs exhibit spontaneous homeotropic alignment in a confined cell without using additional pretreatment for LC alignment.<sup>[9]</sup> Although it is a significant advance for a cost-effective manufacture, there are critical hurdles to overcome such as notorious aggregation issues of nano-sized particles, uniformity, and reliability of the alignment due to a weak adsorption and migration of nano-particles.

Here, a completely different approach has been proposed. We report a novel technique for a uniform, reliable, and cost-effective method for a homeotropic LC alignment. By using a small amount of azo-dye doped to a nematic host (i.e., alignment agent and LC host contained in the same vessel, so called "one-bottle approach"), high quality homeotropic alignment is achieved without any pretreatment of substrates for LC alignment and without compromising physical properties of a host LC. In situ photoirradiation of the dye-doped nematic host, confined in a thin cell, results in a spontaneous homeotropic alignment of the nematic host. In this report, we demonstrate the in situ homeotropic alignment of nematic liquid crystal and corresponding mechanism behind the phenomenon. In addition to the optical and electro-optical characterizations, atomic force microscopy (AFM), field emission scanning electron microscopy (FE-SEM), energy dispersive spectrometer (EDS), UV-vis spectroscopy, Fourier transform Infrared spectroscopy (FT-IR), particle size measurement techniques are employed for the study. We strongly believe that a novel concept of "one-bottle approach" effectuated by in situ process for homeotropic LC alignment provides significant advantages over the conventional methods for LC alignment. Furthermore, the proposed mechanism will provide a new insight on liquid crystal alignment which would lead to exciting researches in future.

Our new approach begins with a nematic LC mixture doped with a small amount of photochromic azo-dye. Two different

Dr. S. Kundu, Prof. S. H. Lee, Prof. S.-W. Kang  
Department of BIN Fusion Technology  
Chonbuk National University  
Jeonju, 561-756, Korea  
E-mail: swkang@jbnu.ac.kr  
Prof. M.-H. Lee  
The Graduate School of Flexible and Printable Electronics  
Chonbuk National University  
Jeonju, 561-756, Korea  
E-mail: lsh1@jbnu.ac.kr



DOI: 10.1002/adma.201300730

compounds with an azo-benzene component are used independently as a dopant: 4-hydroxy-4'-buthyl diazobenzene (Dye-1, see Supporting Information, Figure S1) and relatively more elongated and symmetric bis(4-azobenzoic acid-4'-n-octyloxyphenyl ester) (Dye-2, Figure 3a, see also Supporting Information, Figure S1). The Dye-1 crystal melts to isotropic liquid at 82.4 °C without showing mesomorphic phase. The Dye-2 exhibits Smectic A phase from 152.0 °C and melts to isotropic liquid at 302.0 °C. <sup>1</sup>H-NMR spectroscopy data and phase sequences of the dye molecules are shown in the Supporting Information. Indium-tin-oxide (ITO) coated glass substrates were used without any treatment for LC alignment. Both electro-optic (E.O.) LC cells loaded with different dyed mixtures exhibit an initial random planar alignment as expected. Subsequent UV-irradiation with a photomask results in a homeotropic alignment for the Dye-2 mixture while no significant change is observed for the Dye-1 mixture. **Figure 1a** and **1b** display macroscopic images of the cell with the Dye-2

under crossed polarizers. The cell exhibits a planar alignment through a whole active area as shown in Figure 1a. The UV-irradiated area turns into a dark circle as seen in Figure 1b. The corresponding polarized optical microscopy (POM) and conoscopy images in Figure 1c and 1d clearly illustrate the transition from a random planar to homeotropic alignment upon UV-exposure. Essentially the same anchoring transition is observed for different concentrations of the Dye-2 ranging 0.1 to 1.0 wt%. The effective concentration is very low so that the physical properties of a host LC, initially optimized for device applications, are not hampered by the dopant. The electro-optic responses shown in Figure 1e and 1f present a typical behavior of the vertically aligned nematic LC cell which is dominantly adapted for LCD TVs. Both voltage-to-transmittance curve (*V*-*T*) and grey-to-grey response time for both rising and decaying exhibit accomplished characteristics. The homeotropic state induced by UV-irradiation shows a good temperature stability. It retains a dark homeotropic state after heating the cell above nematic-to-isotropic transition temperature at 100 °C for 24 hours. The anchoring transition caused by UV-light is irreversible under visible light (430–450 nm wavelength) irradiation. It is also noteworthy that the Dye-2 doped mixture with LC cells consisted of bare-glass, polyimide, or polystyrene coated substrates exhibit essentially the same anchoring transition phenomenon.

To understand the origin of anchoring transition effect, we have performed several experiments by using 0.5 wt% Dye-2 doped samples. First, the homeotropic samples after UV-irradiation have been immersed into excess amount of hexane to selectively remove LC host. After complete removal of LCs, a few different fresh LCs, without a dye additive, have been reloaded. All LC mixtures, regardless of positive or negative dielectric anisotropy, show essentially the same alignment of LC molecules as in the initial irradiated cell (see Supporting Information, Figure S2). Therefore, it is evident that the anchoring transition occurs through the surface-induced phenomenon during the UV-irradiation and the modified surface is stable against solvent treatment.

Second, we have investigated inner surfaces of the cell after removal of LCs by using AFM, FE-SEM, and EDS. **Figure 2** represents selected AFM and SEM images for the top and bottom surfaces of UV-irradiated area and pristine ITO-surface. As seen in Figure 2a–c and d–f, the microscopic structures are formed on both top and bottom inner surfaces in the exposed area. Relatively thicker layer with a rough surface has been deposited on near UV-side (top) surface compared to the opposite surface. This is presumably due to the intensity gradient of UV-light inside the LC cell. For the bottom surface, approximately

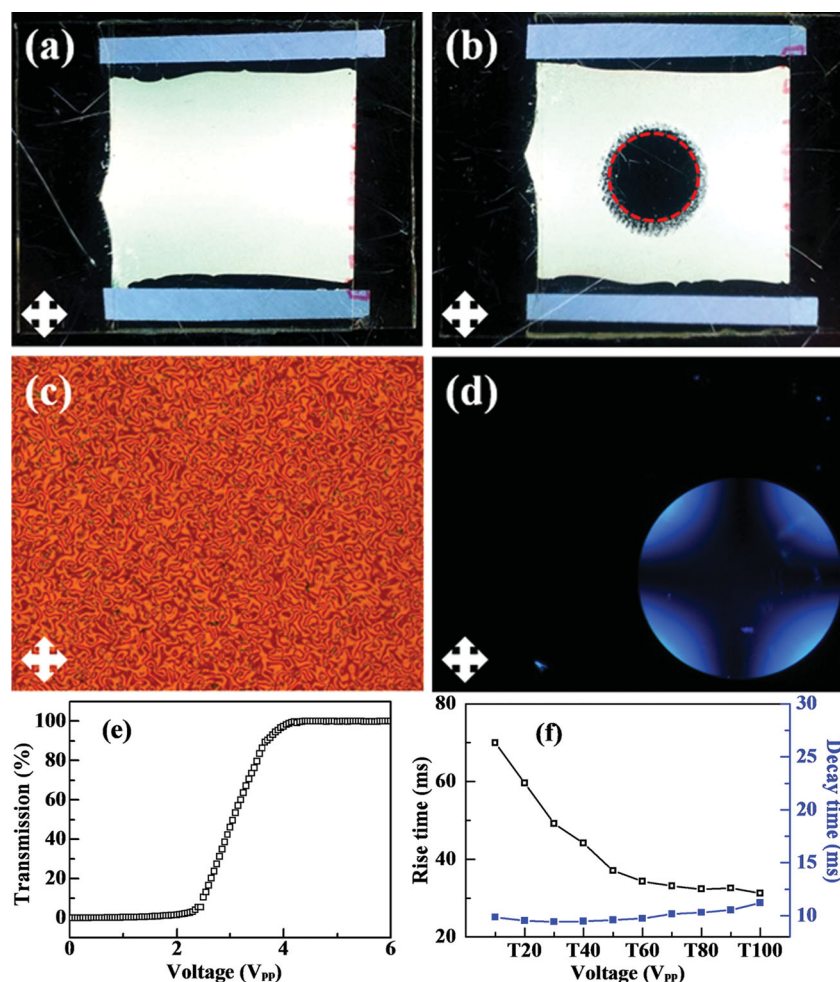


**Figure 1.** Depolarized optical images and electro-optical response of the Dye-2 doped nematic mixture: a,b) the macroscopic figures before (a) and after (b) UV-irradiation with a mask; c,d) the corresponding microscopic images exhibiting random planar (c) and homeotropic (d) states and (inset) a conoscopic figure for the exposed area. The UV-exposed area is marked by a red circle. e,f) The voltage–transmission (*V*-*T*) curve and grey-to-grey response time for both rising and decaying measured from 4 μm thick E.O. cell, respectively.

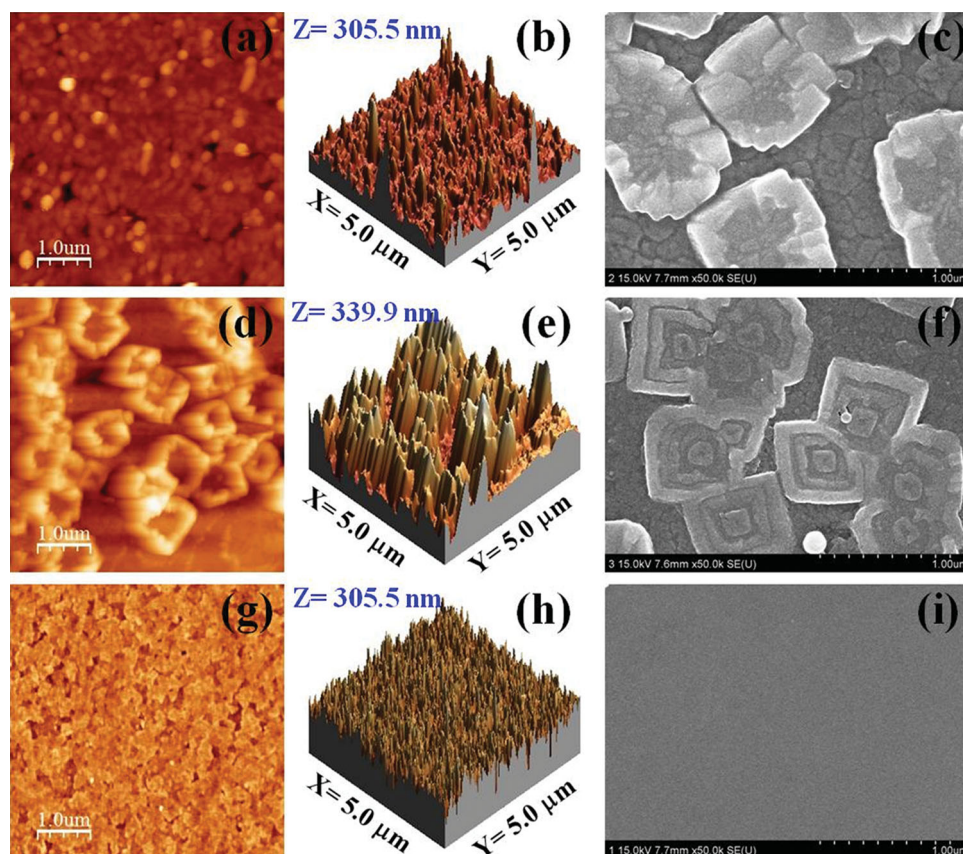


**Figure 2.** AFM and FE-SEM micrographs of the inner surfaces of the UV-irradiated LC cell and bare ITO glass: (a–c) represent the AFM image, a 3D view of the surface, and the FE-SEM image from the top substrate of the UV-irradiated region. d–i) The corresponding images for the bottom substrate of the UV-irradiated area (d–f) and the ITO-surface of the unexposed area (g–i).

micrometer sized flower-like structure is observed. The incoherent structures are formed on a thin continuous layer. In both cases, the surface topography becomes much rougher than the pristine ITO-surface. The scale of the z-axis in Figure 2b and 2e is at least 50 times larger than that in Figure 2h. The corresponding values of root mean square (RMS) roughness are 22.8, 54.4, and 0.6 nm, respectively (see Supporting Information, Figure S3 for the statistical data of each AFM image). We conjecture that the roughened surfaces formed by the deposition of dye molecules are responsible for a homeotropic alignment of LCs.

The EDS data collected from each surface show a clear difference. The existence of a carbon (C) and nitrogen (N) atoms is evident for the top and bottom surfaces of UV-irradiated substrates while no subsistence of C and N atoms is observed for a clean ITO-surface (see Table S1–3 in the Supporting Information for details). Therefore, it is reasonable to conclude that the microscopic structures on the UV-irradiated surface are put together from the Dye-2 molecules. The dye molecules form agglomerates and deposit on the inner surface of the LC cell. The structures on FE-SEM images in Figure 2c and 2f are more perceptible and provide more detailed information. The square-shape morphology strongly indicates a crystalline nature of the dye agglomerates assembled on a continuous layer of azo-dye molecules. Additional SEM images are presented in Figure S4 in the Supporting Information, for more information.

The arising question is how the Dye-2 molecules are put together into crystalline aggregates and deposited on the surfaces. To investigate this object, FTIR spectra have been taken for a melt film of the Dye-2 on a silicon wafer and a deposited layer on a silicon wafer prepared in a LC host under UV-irradiation. The results shown in Figure S5 in the Supporting Information are virtually the same which may indicate no chemical reaction such as polymerization or degradation of the dye molecules during the crystal formation. It is also confirmed that the crystal can be melted by heating and UV-vis absorption spectrum changes as a result of it. Based on these results, we conjecture that the dye molecule retains its identity and photochromic isomerization is responsible for the crystallization of the dye molecules. As well known, the azo-benzene chromophore exhibits *trans-cis* isomerization as represented in Figure 3a for the Dye-2 molecule. In general, the process is reversible. It is open reported that the dipole moment (represented by the blue arrows) in *cis*-configuration is several folds larger than that in *trans*-form due to the broken symmetry. As a result of the augmented dipole moment, the *cis*-form dye molecules pack together, form crystalline agglomerates, and deposit on the surface.<sup>[10,11]</sup> It should be noted that the relatively smaller Dye-1 molecules in both *trans*- and *cis*-form dissolve very well in the LC host. Therefore, it cannot form solid aggregates at a low concentration and be deposited on the surface, and consequently

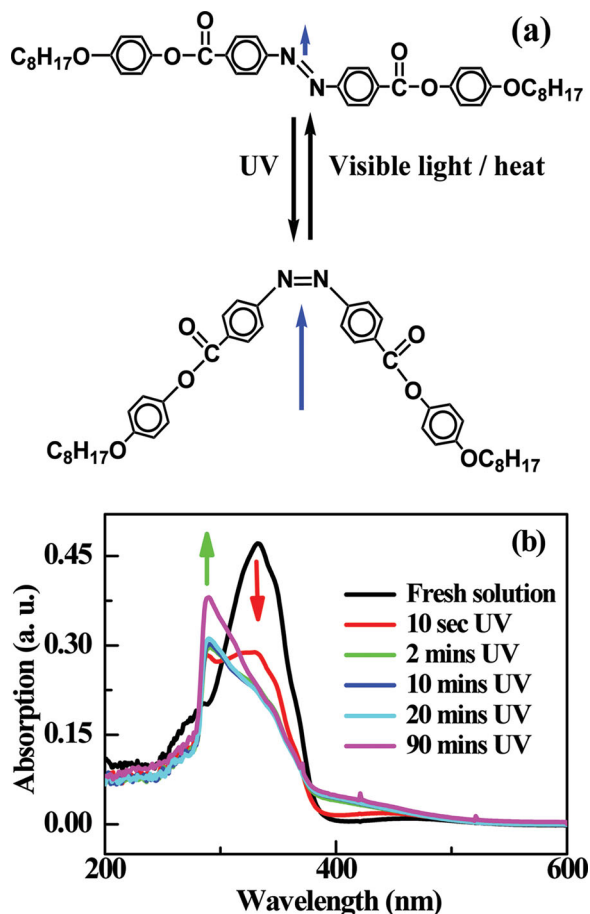


**Figure 3.** Molecular structure, *trans*- to *cis*-isomerization of the Dye-2 molecule, and corresponding UV-vis absorption spectra as a function of UV-irradiation time: a) molecular structures of the Dye-2 in its *trans*- and *cis*-configuration and isomerization process. The magnitude of the dipole moment is qualitatively proportional to the length of the blue arrows. b) The UV-vis absorption spectra of the 0.01 mM Dye-2 in chloroform solution with respect to the UV-irradiation time. The UV-irradiation time is indicated in the legend.

cannot induce the anchoring transition as mentioned earlier. On the other hand, the Dye-2 molecules have limited solubility in solvents. No more than  $\approx 2.0$  wt% dissolve in a host LC due to its symmetric molecular structure with a large elongation of a hard-core. It seems that a blue shift of the UV-vis absorption peak with a comparatively narrower band as seen in Figure 3b is attributed to the limited solubility. In this case, the increased dipole moment (approximately up to 4 Debye) can facilitate crystalline agglomeration of *cis*-form molecules.<sup>[11]</sup> Figure 3b presents the UV-vis absorption changes of a 0.01 mM Dye-2 solution in chloroform with respect to UV-irradiation time. The fresh solution shows a strong peak at 322 nm and weak peak at 469 nm corresponding to the  $\pi$ - $\pi^*$  transition of *trans*-form isomer and  $n$ - $\pi^*$  transition of *cis*-form isomer, respectively.<sup>[12]</sup> Upon UV-irradiation the strong peak rapidly diminishes and a new peak arises at 289 nm attributed to the side by side stacking of *cis*-isomers due to a strong dipole moment. This peak is intensified by the prolonged exposure time. The significant

blue shift of absorption peaks for crystalline chromophore has been previously reported in ref.<sup>[12]</sup> UV-light induced *trans*- to *cis*-isomerization increases a population of *cis*-isomer and consequently expedites aggregation to form a crystal. This inference is corroborated by the experiment of particle size analysis performed before and after UV-exposure. The accelerated formation of azo-dye aggregates in *cis*-configuration is also recently reported in ref.<sup>[10,11]</sup>

Interestingly, in our case, the *cis*-form crystals are not converted to *trans*-isomer by the visible light irradiation. However, thermal treatment to its melting temperature instigates relaxation back to the *trans*-isomer. The UV-vis spectra measured after melting the *cis*-form crystal clearly demonstrate a thermal conversion from *cis*- to *trans*-isomer. The solid aggregates readily dissolve in solvent after annealing the crystal at above melting temperature (180 °C for 1 hour). The UV-vis absorption spectrum taken at room temperature after annealing and dissolving in chloroform shows a complete recovery of the absorption peak at 322 nm, corresponding to the absorption of *trans*-isomer (see Supporting Information, Figure S6). This substantiates our assumption for the photoisomerization initiated assembly of the dye molecules rather than the polymerization induced phase separation. This is further corroborated by the particle size analysis performed before and after the UV-exposure of Dye-2 solution in chloroform. One hour UV-irradiation to a fresh solution with no measurable particles cultivates a more light scattering state due to the particle formation. The average particle size is 2.8  $\mu\text{m}$  with a count rate of 606 kcps (see Supporting Information, Figure S7 for details). Therefore, it is evident that the agglomeration of *cis*-form isomers develops prior to a deposition at the solid surface.

Based on the results discussed above, we conclude that the *trans*- to *cis*-isomerization and remarkably larger dipole moment of the *cis*-isomer are the primary factor for a crystallization of azo-Dye-2 molecules under UV-exposure. The resulting dye agglomerates formed in a bulk LC under UV-light irradiation are drawn by the liquid-solid interface (i.e., so-called "Pickering effect") and self-assemble into a unique crystal structure at the solid surface. This significantly alters topography of surfaces and form roughened surfaces as seen by the AFM and FE-SEM images in Figure 2. The topographical modification of a surface, induced by the azo-dye doped LC mixture under UV-irradiation, plays a critical role for the anchoring transition from the initial planar to homeotropic state of host liquid crystals.

The crucial question is why LC molecules anchor vertically at the dye deposited surfaces. It is well known and generally accepted that one dimensional topographic pattern such as a grooved surface aligns LC director parallel to the smoother direction (i.e., along the groove direction).<sup>[2]</sup> In this case, mainly physical interaction between elastic LC medium and patterned solid surface is the primary driving force for a uniform LC alignment in the plane of the solid surface. The 2D-topographic patterns have also been reported for a homeotropic alignment. The 2D-structured surfaces with pillars, posts and wells can align LC director vertical to the surface.<sup>[6]</sup>

In our case of dye deposition, presumably the same physical interaction is the primary driving force for a homeotropic alignment rather than the chemical interaction stemming from the chemical anisotropy of a surface. In general, calamitic LC

molecules prefer to anchor tangentially on the smooth surface as on the ITO-surface illustrated in **Figure 4a**. No specific in-plane orientation of the director (represented by a green arrow) is preferred if the surface anisotropy is not imposed by external treatments. However, the in-plane alignment of a LC director in any direction on the rough surface causes a high elastic distortion of LC medium. **Figure 4b** presents a cross-sectional profile of the dye deposited surface (illustrated by orange color), planar anchored LC molecules at the surface, and consequent

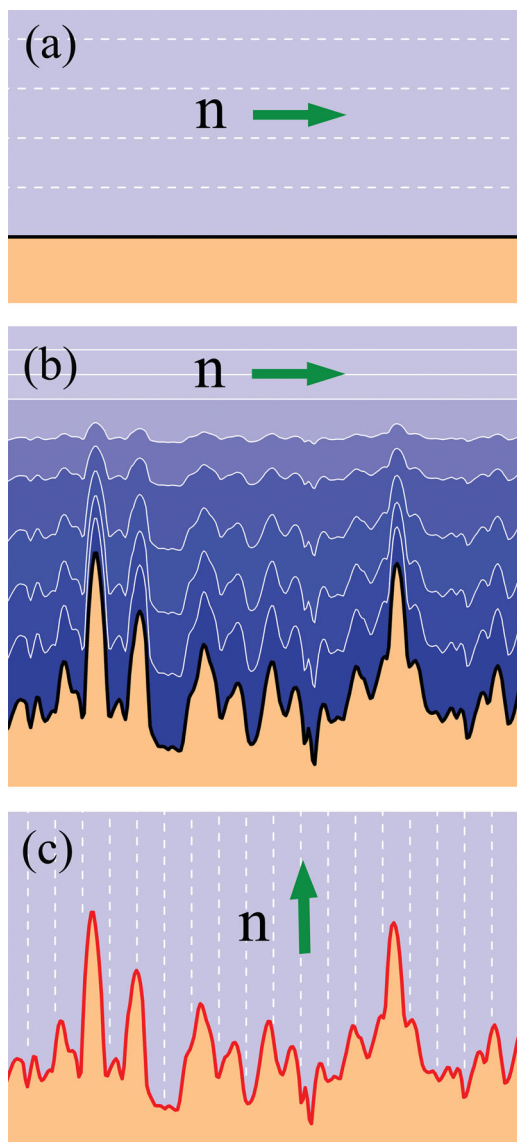


**Figure 4.** Graphical illustration of the LC alignment at solid surfaces with different roughnesses: a) planar alignment on a smooth surface, b) planar alignment with a high elastic distortion, and c) homeotropic alignment with a minimum distortion on a rough surface. The LC molecules align tangentially to the white lines, and the average nematic director is indicated by the green arrow. The cross-section of each surface is shown as an orange color and the color contour in blue represents the degree of elastic deformation of LC molecules. The darker color indicates higher distortion and the lightest color corresponds to the minimum elastic energy.

large elastic deformation of LCs. The LC molecules align tangential to the white lines. The color contour in blue represents a degree of elastic deformation of the LC medium. The darker indicates the higher distortion and the lightest corresponds to a minimum elastic energy. To avoid a highly distorted state at a rough surface, the LC molecules prefer to align vertically to the surface to minimize elastic distortion and subsequently minimize total free energy of the system. **Figure 4c** shows a homeotropic alignment of LC director at a rough surface and minimized elastic deformation of LC molecules as represented by lightest blue. The elastic energy of a LC medium competes with the interaction energy between LCs and surface. For a planar anchoring on smooth surfaces, the interaction energy efficiently overcomes imperceptible elastic deformation. For a rough surface, however, elastic energy predominates and thus the director escapes to a vertical direction. For a planar alignment on the rough surface, the elastic energy critically depends on roughness of surface especially the average height of the peaks and the average inter-distance between peaks. Accordingly, degree of roughness, height-to-distance ratio, molecular dimension and elastic constant of LCs are crucial parameters to determine an anchoring condition for either planar or vertical alignment of LC director. Although the topography of dye deposited surfaces observed in our study is irregular, the height-to-distance ratio seems to satisfy the conditions for a homeotropic alignment of conventional LCs.

We have demonstrated reliable, practical and cost-effective “one-bottle approach” for a homeotropic alignment of nematic liquid crystals. In situ homeotropic alignment is achieved by photochromic *trans*- to *cis*-isomerization of the azo-dye doped in a nematic host. The augmented dipole moment of a *cis*-isomer formed under UV-irradiation expedites a molecular assembly into crystalline aggregates. Subsequent deposition of the aggregates creates roughened surface and induces anchoring transition from the initial planar to homeotropic alignment of LCs. In our method, it is experimentally supported that the surface modification is achieved through an interfacial self-assembly of the dye aggregate instead of molecular adsorption due to a dipole-dipole interaction or hydrogen bonding between solid surface and LC molecules. The offered method provides a stable LC alignment which is an essential requirement for device applications. The alignment is unwavering against temperature, light and chemical treatment and therefore practically permanent for a device implementation. We propose that the origin of anchoring transition is attributed to the physical interaction between elastic LC medium and roughened surface rather than a chemical interaction due to the anisotropy in molecular orientation at the surface. Our work will provide a new insight on liquid crystal alignment which would lead to exciting researches in future. Simple but reliable “one-bottle approach” not only provides an intuitive understanding for LC alignment at surfaces but also is a promising technique for practical device applications.

## Experimental Section

**Materials:** Nematic liquid crystals with either positive (E7, Merck) or negative (LC-1 and LC-2, Merck) dielectric anisotropy are used as

a host liquid crystal. The specifications of LC material are provided in the supporting information. Two photochromic azo-dye molecules, 4-hydroxy-4'-butyl diazobenzene (Dye-1 shown in Supporting Information, Figure S1) and bis(4-azobenzoic acid-4'-n-octyloxyphenyl ester) (Figure 3a), are independently used as a dopant. To obtain a homogeneous mixture, 0.1, 0.3, 0.5 and 1.0 wt% dye-molecule added separately to the LC host is melted by stirring at a few degrees above the nematic-to-isotropic transition temperature ( $T_{NI}$ ) of host LCs.

**Sample Preparation:** To fabricate electro-optic LC cells, either bare ITO-coated glass or ITO-coated glass with a conventional polyimide deposition were used as substrates. The cell gap was maintained by 10  $\mu\text{m}$  thick tape spacers or silica-ball spacers with 4  $\mu\text{m}$  diameter. The dye-doped mixtures were loaded into the cells with a capillary action at 5 degree above the  $T_{NI}$  and slowly cooled to an ambient temperature. The planar aligned nematic cells were covered with a black mask with a 5 mm circular hole and subsequently exposed to UV-light with 500  $\text{mW cm}^{-2}$  intensity for 30 minutes. The Spot Cure Model SP-9 (Ushio Inc.) was used for UV-source and a mirror was kept beneath the cell during the vertical irradiation. To selectively dissolve the LC host, the cells were immersed in excess amount of hexane for 24 hours and dismantled to examine the surface with the AFM, FE-SEM, EDS, FTIR and UV-vis spectroscopy. For particle size analysis and UV-vis spectroscopy, various concentrations of dye-solutions in chloroform or liquid crystal were prepared. The drop cast films of dye in chloroform solution and melt films of solid dye on the quartz plate are also prepared for the UV-vis spectroscopy. The hybrid cells with quartz plate and silicon wafer were fabricated for the UV-vis and FTIR spectroscopy.

**Measurements:** POM and conoscopic images were taken using an Nikon Eclipse LV 100 POL polarizing optical microscope equipped with a Nikon DS-Ri1 CCD camera and an Instec STC 200 temperature controller with Instec HCS 402 hot stage. Atomic force microscopy was performed on SPM Nano Focus n-Tracer. FE-SEM and EDS were carried out using the Hitachi S-4800 high resolution SEM. The UV-vis absorption spectra of the dye solutions in LC or chloroform were measured by the UV-vis spectrophotometer (Jasco, ARSN-733). For particle size analyses, count rate and particle size of the dye-solutions in chloroform contained in a quartz cuvette were measured as a function of UV-irradiation time using a Brook Haven BioPlus particle size analyzer (Brookhaven Inc.). FTIR spectra of azo-dye deposited on silicon wafer were recorded prior to and after UV-irradiation using FT-IR 4200 (Jasco, Japan). Electro-optical switching behaviors are characterized by LCMS-200 (Sesim Photonics Technology, Korea).

## Supporting Information

Supporting Information is available from the Wiley Online Library or from the author.

## Acknowledgements

This research was supported by the World Class University program funded by the Ministry of Education, Science and Technology through the National Research Foundation of Korea (R31-20029). The authors thank Dr. Yong-Kuk Yun and Dr. Dong-Mee Song from Merck Advanced

Technologies in Korea for their kind support of LC materials and useful discussions.

Received: February 14, 2013

Published online:

- [1] M. Hasegawa, in *Alignment Technologies and Applications of Liquid Crystal Devices*, (Eds: K. Takatoh, M. Hasegawa, M. Koden, N. Otoh, R. Hasegawa, M. Sakamoto), Taylor and Francis, New York, USA, **2005**, Ch. 2 and Ch. 3.
- [2] a) D. W. Berreman, *Phys. Rev. Lett.* **1972**, *28*, 1683; b) S. Kumar, J.-H. Kim, Y. Shi, *Phys. Rev. Lett.* **2005**, *94*, 077803; c) J. Fukuda, M. Yoena, H. Yokoyama, *Phys. Rev. Lett.* **2007**, *98*, 187803; d) J. Fukuda, M. Yoena, H. Yokoyama, *Phys. Rev. Lett.* **2007**, *99*, 139902.
- [3] K.-H. Kim, J.-K. Song, *NPG Asia Mater.* **2009**, *1*, 29.
- [4] a) V. K. Gupta, N. L. Abbott, *Science* **1997**, *276*, 1533; b) R. R. Shah, N. L. Abbott, *Science* **2001**, *293*, 1296.
- [5] a) S. M. Malone, D. K. Schwartz, *Langmuir* **2008**, *24*, 9790; b) V. K. Gupta, N. L. Abbott, *Phys. Rev. E* **1996**, *54*, R4540.
- [6] a) Y. Yi, G. Lombardo, N. Ashby, R. Barberi, J. E. MacLennan, N. A. Clark, *Phys. Rev. E* **2009**, *79*, 041701; b) S. Kiston, A. Geisow, *Appl. Phys. Lett.* **2002**, *80*, 3635; c) S. Lazarouk, A. Muravski, D. Sasinovich, V. Chigrinov, S. S. Kwok, *Jpn. J. Appl. Phys.* **2007**, *46*, 6889.
- [7] K. Ichimura, *Chem. Rev.* **2000**, *100*, 1847.
- [8] W. M. Gibbons, P. J. Shannon, S.-T. Sun, B. J. Swetlin, *Nature* **1991**, *351*; b) C. Ruslim, L. Komitov, Y. Matsuzawa, K. Ichimura, *Jpn. J. Appl. Phys.* **2000**, *39*, L104; c) L. Komitov, K. Ichimura, A. Strigazzi, *Liq. Cryst.* **2000**, *27*, 51.
- [9] a) S.-C. Jeng, C.-W. Kuo, S.-L. Wang, C.-C. Liao, *Appl. Phys. Lett.* **2007**, *91*, 061112; b) H. Qi, B. Kinkead, T. Hegmann, *Adv. Funct. Mater.* **2008**, *18*, 212; c) D. Zhou, W. Zhou, X. Cui, L. Guo, H. Yang, *Adv. Mater.* **2011**, *23*, 5779; d) L. Wang, W. He, X. Xiao, F. Meng, Y. Zhang, P. Yang, L. Wang, J. Xiao, H. Yang, Y. Lu, *Small* **2012**, *8*, 2189; e) L. Wang, W. He, X. Xiao, M. Wang, M. Wang, P. Yang, Z. Zhou, H. Yang, H. Yu, Y. Lu, *J. Mater. Chem.* **2012**, *22*, 19629.
- [10] a) M. Grzelczak, J. Vermant, E. M. Frust, L. M. Liz-Marzan, *ACS Nano* **2010**, *4*, 3591; b) M. Fialkowski, K. J. M. Bishop, R. Klajn, S. K. Smoukov, C. J. Campbell, B. A. Grzybowski, *J. Phys. Chem. B* **2006**, *110*, 2482.
- [11] a) X. Tong, G. Wang, Y. Zhao, *J. Am. Chem. Soc.* **2006**, *128*, 8746; b) X. Tong, M. Pelletier, A. Lasia, Y. Zhao, *Angew. Chem. Int. Ed.* **2008**, *47*, 3596; c) H. S. Lim, W. H. Lee, S. G. Lee, D. Lee, S. Jeon, K. Cho, *Chem. Commun.* **2010**, *46*, 4336; d) K. Ichimura, S. Oh, M. Nakagawa, *Science* **2000**, *288*, 1624.
- [12] a) Z. Sekkat, J. Wood, W. Knoll, *J. Phys. Chem.* **1995**, *99*, 17226; b) H. H. Jaffe, S. J. Yeh, R. W. Gardener, *J. Mol. Spectrosc.* **1958**, *2*, 120; c) T. Seki, K. Ichimura, *Thin Solid Films* **1989**, *179*, 77; d) T. Sato, Y. Ozaki, K. Iriyama, *Langmuir* **1994**, *10*, 2363; e) Y. Wang, Q. Li, *Adv. Mater.* **2012**, *24*, 1926; f) Q. Li, Y. Li, J. Ma, D.-K. Yang, T. J. White, T. J. Bunning, *Adv. Mater.* **2011**, *23*, 5069; g) Y. Wang, A. Urbas, Q. Li, *J. Am. Chem. Soc.* **2012**, *134*, 3342.